Floxed exon (Flexon): A flexibly positioned stop cassette for recombinase-mediated conditional gene expression

Justin M. Shaffer[a] and Iva Greenwald[a,1]

[a]Department of Biological Sciences, Columbia University, New York, NY 10027

Contributed by Iva Greenwald; received September 22, 2021; accepted December 4, 2021; reviewed by John Kim, Barth Grant, and Ann Rougvie

Conditional gene expression is a powerful tool for genetic analysis of biological phenomena. In the widely used "lox-stop-lox" approach, insertion of a stop cassette consisting of a series of stop codons and polyadenylation signals flanked by *lox* sites into the 5′ untranslated region (UTR) of a gene prevents expression until the cassette is excised by tissue-specific expression of Cre recombinase. Although lox-stop-lox and similar approaches using other site-specific recombinases have been successfully used in many experimental systems, this design has certain limitations. Here, we describe the Floxed exon (Flexon) approach, which uses a stop cassette composed of an artificial exon flanked by artificial introns, designed to cause premature termination of translation and nonsense-mediated decay of the mRNA and allowing for flexible placement into a gene. We demonstrate its efficacy in *Caenorhabditis elegans* by showing that, when promoters that cause weak and/or transient cell-specific expression are used to drive Cre in combination with a *gfp(flexon)* transgene, strong and sustained expression of green fluorescent protein (GFP) is obtained in specific lineages. We also demonstrate its efficacy in an endogenous gene context: we inserted a *flexon* into the Argonaute gene *rde-1* to abrogate RNA interference (RNAi), and restored RNAi tissue specifically by expression of Cre. Finally, we describe several potential additional applications of the Flexon approach, including more precise control of gene expression using intersectional methods, tissue-specific protein degradation, and generation of genetic mosaics. The Flexon approach should be feasible in any system where a site-specific recombination-based method may be applied.

conditional gene expression | lox-stop-lox | stop cassette | *C. elegans* | tissue-specific RNAi

Conditional gene expression is an important tool for understanding how genes and proteins function in different tissues, lineages, and stages of development in complex organisms. Traditionally, control of gene expression is achieved by using regulatory regions derived from genes that are expressed in specific spatial and temporal patterns. However, the characterized regulatory regions do not always have the ideal expression pattern, and often trade-offs must be made between expression level and spatiotemporal specificity.

To address some of these limitations, we devised a variation on the stop cassette, a sequence that inhibits expression that can be removed by tissue-specific drivers of site-specific recombinase systems. In the widely used lox-stop-lox system, the stop cassette generally consists of tandemly repeated polyadenylation signals flanked by *lox* target sequences of Cre recombinase, that is inserted into the 5′ untranslated region (UTR) of a gene of interest; tissue-specific expression of Cre leads to excision of the cassette to restore gene expression (1–5) (Fig. 1*A*). Similar stop cassettes have also been used with the Flp/*frt* system (6, 7), and variations include the coding region for a selectable or visible marker within the cassette for easy identification of recombination events (5, 8–15). In all of these cases, the stop cassette causes a transcriptional stop prior to the first exon, blocking expression of the gene, but when the recombinase is provided through a separate driver, the cassette is excised and the gene of interest is expressed. Stop cassettes are used in transgenes to generate spatiotemporal specificity via tissue-specific recombinase drivers by placing the cassette between the coding region and a strong promoter. For example, conditional control of transgene expression has been accomplished in mice by inserting transgenes with stop cassettes into the ROSA26 locus, a neutral locus with the potential for midlevel expression in multiple tissues after Cre-mediated excision of the stop cassette (16–20).

Stop cassettes that rely on transcription termination share certain limitations. Unwanted expression of the gene can occur from incomplete abrogation of transcription and translational initiation downstream of the stop cassette. Leaky expression has also been observed from read-through transcription that results from incomplete recombination between sequence repeats within the stop cassette (21). While leaky expression is the chief concern for stop cassette usage in transgenes, further limitations apply when using a stop cassette in an endogenous context. Different isoforms of a gene may have varying start sites, potentially complicating the application of lox-stop-lox to create likely null alleles. In addition, the 5′ UTR may also contain uncharacterized but important regulatory sequences; in *Caenorhabditis elegans*, these could include trans-splicing signals upstream of conventional genes and internal to operons (reviewed in ref. 22). Placing

Significance

Tools that afford spatiotemporal control of gene expression are crucial for studying genes and processes in multicellular organisms. Stop cassettes consist of exogenous sequences that interrupt gene expression and flanking site-specific recombinase sites to allow for tissue-specific excision and restoration of function by expression of the cognate recombinase. We describe a stop cassette called a *flexon*, composed of an artificial exon flanked by artificial introns that can be flexibly positioned in a gene. We demonstrate its efficacy in *Caenorhabditis elegans* for lineage-specific control of gene expression and for tissue-specific RNA interference and discuss other potential uses. The Flexon approach should be feasible in any system amenable to site-specific recombination-based methods and applicable to diverse areas including development, neuroscience, and metabolism.

Author contributions: J.M.S. designed research; J.M.S. performed research; J.M.S. analyzed data; J.M.S. and I.G. wrote the paper; and I.G. supervised research.

Reviewers: J.K., Johns Hopkins University; B.G., Rutgers The State University of New Jersey; and A.R., University of Minnesota Twin Cities.

The authors declare no competing interest.

[1]To whom correspondence may be addressed. Email: isg4@columbia.edu.

This article contains supporting information online at http://www.pnas.org/lookup/suppl/doi:10.1073/pnas.2117451119/-/DCSupplemental

Published January 13, 2022.

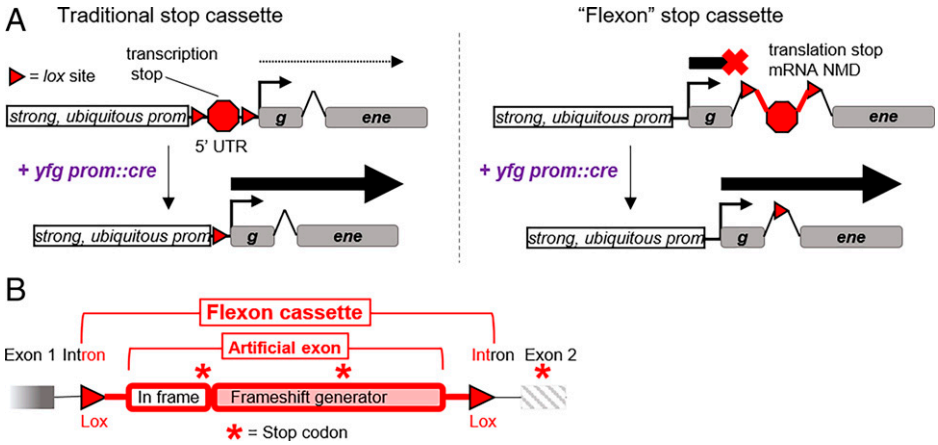

Fig. 1. Design and use of a Floxed exon cassette (*flexon*). (*A*) A traditional stop cassette (*Left*) is placed in the 5′ UTR of the gene of interest and designed to block gene expression through a transcriptional stop. A *flexon* stop cassette (*Right*) is designed to abrogate gene expression by a translational stop and frameshift mutations leading to stop codons in other frames, and is also expected to result in nonsense-mediated decay (NMD) of the mRNA. Further differences are discussed in the text. Both traditional and *flexon* stop cassettes may use strong, ubiquitous promoters to drive expression in specific lineages or tissues after cassette excision by Cre recombinase driven by the promoter of "*your favorite gene*" (*yfg*). (*B*) In this study, the artificial exon of the *flexon* has an in-frame, three-codon leader sequence that ends with an in-frame stop codon followed by a frameshift-generating sequence that creates additional premature stop codons in all frames. The *flexon* used in this study is bounded by *lox2272* sites. Specific parameters may be varied as described in the text and *SI Appendix*.

a stop cassette into these sequences could alter expression of the downstream gene; even after the cassette is excised, the *lox* scar could disrupt important regulatory sequences.

Here, we outline a strategy for a stop cassette that increases insertion site flexibility for both transgenes and endogenous genes, while retaining spatiotemporal control of expression. We call this strategy "Flexon," for "Floxed exon," in which we engineer a stop cassette that includes an artificial exon designed to prevent protein translation by causing premature termination in all three reading frames and to trigger nonsense-mediated decay of the mRNA that contains it. A *flexon* can be inserted into an intron or exon of a gene, providing different options for its placement within a transgene or endogenous locus. We demonstrate the efficacy of the Flexon approach for creating bright lineage markers and for abrogating function of an endogenous Argonaute gene to allow restoration of function for tissue-specific RNA interference (RNAi) and describe other potential applications of Flexon for genetic analysis.

Results

General Design Considerations. As with other stop cassettes, the principle behind the *flexon* is that it should prevent target gene expression in the absence of tissue-specific recombinase-mediated excision. In addition, the *flexon* is designed to be versatile regarding where it can be inserted in an open reading frame and prevent ectopic gene expression due to spurious initiation downstream of the cassette. Furthermore, although we have used *Cre-lox* in this study, the Flexon approach is compatible with any site-specific recombination system. We note that with regard to nomenclature, we use "Flexon" to describe the approach and "*flexon*" for the cassette used to create a new genotype.

Any *flexon* contains an artificial exon with one or more stop codons flanked by artificial introns (Fig. 1 A and B). Each flanking intron of the cassette contains a single *lox* site, and both *lox* sites are oriented in the same direction to allow for excision of the stop sequence in the exon (23). Due to the flanking introns, the stop sequence is spliced into the transcript if the cassette is inserted into an exon or an intron, allowing for flexible placement within the gene of interest (Fig. 1*A*).

A *flexon* is designed to block gene expression at the level of translation instead of transcription. The artificial exon contains redundant mechanisms designed to halt translation of the protein: it contains stop codons both in frame and out of frame, relative to the gene of interest, and creates a frameshift that introduces additional stop codons downstream (Fig. 1*B*). Since the *flexon* exon is a single, short, nonrepetitive sequence, it is relatively easy to clone and adjust (*SI Appendix*) and presumably would not be subject to incomplete recombination of repetitive stop sequences (21). If the initial premature stop is read through, the subsequent frameshift mutations would be expected to create a nonfunctional protein. Furthermore, it would be expected to trigger nonsense-mediated decay (NMD) of the mRNA as a further guarantee against producing a protein. We note that in order to trigger NMD, premature stop codons need to be at least 50 nucleotides upstream of the final exon junction (24, 25). When Cre-mediated recombination occurs, the exon with the stop sequence is removed from the DNA sequence, leaving a single artificial intron with a *lox* scar in the middle and restoring the reading frame to encode for a functional protein (Fig. 1*A*).

Design of the *flexon* Cassette Used in This Study. In the test cases here, we used a *flexon* with the following sequence elements (Fig. 1*B*). Design considerations that may apply to other *flexon* cassettes are addressed in *Discussion* and in *SI Appendix*.

1) In-frame exon sequence: The exon contains a three-codon leader to a stop codon that is in frame with the coding region of the gene in which it was inserted (Fig. 1*B*).
2) Frameshift-generating exon sequence: We used 62 bp of sequence from the neutral 3′ UTR from *tbb*-2 (26) to cause a frameshift of the downstream coding region (Fig. 1*B*). The total length of the exon sequence is the same as the second exon in a widely used, artificial intron-containing form of the coding region of green fluorescent protein (*gfp*) (23) to ensure it is of sufficient length to be spliced into the mRNA. The length of the exon was kept as small as possible to ensure efficient Cre-mediated excision, facilitate cloning, and promote homologous repair for endogenous gene insertion.
3) Intron sequences: The artificial introns were derived from a self-excising drug selection cassette (23). Artificial introns of similar sequences (Fire Vector Kit, 1995) are commonly used for transgenes in *C. elegans* because they demonstrate efficient splicing, due to the short sequence length and canonical splice acceptor and donor sequences.

4) *lox* site selection: We used the *lox* variant *lox2272* to avoid recombination with *loxP* sites in existing transgenes or engineered loci we routinely use in our work.

Using the Flexon Approach in a *gfp(flexon)* Transgene for Strong, Cre-Mediated, Tissue-Specific Expression of GFP. We replaced the first or second intron in codon-optimized *gfp* sequences typically used in *C. elegans* transgenes (*Materials and Methods*) to create "*gfp(flexon)*" sequences (shown schematically in *SI Appendix*, Fig. S1) and used the strong ubiquitous promoter *rps-27p* (27) to drive expression in all somatic cells. The resulting *rps-27p*::*gfp(flexon)* transgenes produce no or minimal visible GFP fluorescence on their own (*SI Appendix*, Fig. S2), indicating little to no ectopic expression in the absence of Cre. We then combined *rps-27p*::*gfp(flexon)* with two different Cre drivers that were made using tissue-specific promoters that drive weak and/or transient expression, as described below. The results were remarkable: The expected lineages were brightly marked throughout larval development (Figs. 2 and 3 and *SI Appendix*, Fig. S3).

The first driver we used would be predicted to result in tissue-specific excision of the *flexon* in all somatic gonadal cells. A *C. elegans* L1 larva hatches with two somatic gonad precursor cells, Z1 and Z4, which generate all of the structures of the somatic gonad during postembryonic development (Fig. 2*A*). During the first phase of gonadogenesis, Z1 and Z4 give rise to 12 cells that form the somatic gonad primordium in the L2 stage, and the somatic gonad blast cells divide in the L3 stage and give rise to many additional cells (28).

The 5′ regulatory region for the *ckb-3* gene, denoted *ckb-3p*, drives expression in the somatic gonad precursor cells Z1 and Z4 in embryos and L1 larvae, but expression rapidly diminishes as the lineage progresses (29). When *ckb-3p* is used to drive 2xNLS::GFP, nuclear GFP is readily visualized in Z1 and Z4 in the L1 stage, but progressively dims and is essentially undetectable by the time the somatic gonad primordium has formed in the L2 stage (Fig. 2 *A* and *B*). The combination of a *ckb-3p::Cre* driver that expresses a form of Cre recombinase optimized for *C. elegans* (30) (*Materials and Methods*) with *rps-27p::2xnls::gfp(flexon)* produces sustained, strong, and specific expression of 2xNLS::GFP in the somatic gonad throughout development (Fig. 2*B* and *SI Appendix*, Fig. S3). Furthermore, when we used a histone tag to stabilize GFP as well as for nuclear localization [*rps-27p::gfp(flexon)::h2b*], fluorescence intensity was sufficient for visualization at lower exposure, and even using a dissecting microscope (Fig. 2 *B* and *C*). Excision frequency approached 100% for both *gfp(flexon)* transgenes; by the time Z1 and Z4 had divided, excision had always been observed.

The second driver we used would be expected to result in tissue-specific excision of the *flexon* in all vulval precursor cells (VPCs). The VPCs are six polarized epithelial cells, named P3.p–P8.p, that are born in the L1 stage and remain quiescent until the L3 stage. At that time, P5.p, P6.p, and P7.p are induced by epidermal growth factor receptor and LIN-12/Notch signaling to adopt vulval fates; the descendants of these cells form the vulval primordium in the L4 stage (31–33). The other VPCs, P3.p, P4.p, and P8.p, do not receive spatial patterning signals and divide once to generate daughter cells that fuse with the major hypodermal syncytium (P3.p sometimes fuses directly, without dividing). A composite regulatory region made from the 5′ flanking region and introns of the *lin-31* gene, called *lin-31p* (34–36) (Fig. 3*A*) displays a dynamic pattern of expression. GFP fluorescence is visible after the cells are born in the late L1 stage and appears uniform in all VPCs during the L2 stage; at the time VPCs commit to their fates in the L3 stage, fluorescence begins to decrease visibly in P5.p, P6.p, and P7.p, and progressively dims and becomes undetectable as their lineages progress (36) (Fig. 3*B*). Fluorescence in P3.p, P4.p, and P8.p remains stronger than in the other VPCs at the beginning of the L3 stage but becomes undetectable after they divide in the L3 stage. By contrast, when *rps-27p*::*2xnls::gfp(flexon)* was combined with a *lin-31p::Cre* driver, GFP was strongly, uniformly, and continuously expressed in the VPCs and their descendants (Fig. 3 *B* and *C*). As in the somatic gonad, the use of a histone tag to stabilize GFP results in fluorescence visible using a dissecting microscope.

Using the Flexon Approach in an Endogenous Gene: An *rde-1(flexon)* Allele Enables Tissue-Specific RNAi. In *C. elegans,* RNAi is usually performed by feeding worms with bacteria that express double-stranded RNA for a gene of interest (37). Tissue-specific RNAi has been accomplished by selectively expressing RDE-1/Argonaute in an *rde-1* hypomorphic or null mutant background (38, 39). As with any other transgenic method, rescue experiments are affected by the strength and specificity of available regulatory regions; for example, our laboratory has had difficulty achieving effective tissue-specific RNAi using *ckb-3p* or *lin-31p* to drive RDE-1 expression in an *rde-1* null mutant background. The transgene-based Flexon approach described above would be one way to circumvent this problem, but for proof of concept to show that a *flexon* works in an endogenous gene context, we created an *rde-1(flexon)* allele that would allow for a physiological level of RDE-1 protein to be restored after tissue-specific, Cre-mediated recombination.

Design of the endogenous* rde-1(flexon) *allele. We used CRISPR-Cas9 to replace the small ninth intron of the endogenous locus of *rde-1* with the same *flexon* cassette used in the *gfp(flexon)* transgenes (Fig. 4*A*). The resulting allele, *rde-1(ar660)*, is hereafter referred to as *rde-1(flexon)*. The position was chosen to disrupt the catalytic PIWI domain, as the goal was to create a sufficiently strong loss-of-function allele that would greatly reduce or eliminate gene activity even if there was a low level of leakiness in this gene context (*Potential Limitations*).

Design of the test of* rde-1(flexon) *for somatic gonad-specific RNAi. To create a strain suitable for somatic gonad-specific RNAi, we combined the endogenous *rde-1(flexon)* allele with the *ckb-3p::Cre* driver described above. The transcription factor HLH-2/E2A, an essential gene for early embryonic development and for gonadogenesis (40), offered an incisive test case. When L4 larvae are fed bacteria expressing double-stranded RNA for *hlh-2* ["*hlh-2(L4-RNAi)*"], all offspring arrest during embryogenesis (41) (Fig. 4*B*). When embryonic lethality is bypassed by feeding L1 larvae with bacteria expressing double-stranded RNA for *hlh-2* ["*hlh-2(L1-RNAi)*"], the treated larvae become sterile adults that lack or have compromised distal tip cells (DTCs), which serve as the germline stem cell niche (42) (Fig. 4*B*); sterility can be readily assessed at the dissecting microscope level. *hlh-2* is also required in the DTCs to lead gonad arm outgrowth in the L3 and L4 stages, so partial loss of function may also be readily assessed by examining the extent of gonad arm outgrowth in adults in the compound microscope. We therefore tested whether *rde-1(flexon)* on its own prevents these deleterious effects of *hlh-2(RNAi)* and whether early lethality is prevented but highly penetrant defects in gonad development result when *rde-1(flexon)* is combined with *ckb-3p::Cre.* We also performed additional supplemental assessments as described below.

rde-1(flexon) *strongly reduces rde-1 activity.* We tested whether inserting a *flexon* into the endogenous *rde-1* gene causes a strong loss-of-function phenotype, a necessary prerequisite for creating a system for tissue-specific RNAi. When we performed *hlh-2(L4-RNAi)* by treating strain N2 (wild type) L4 larvae, all of their progeny arrested during embryogenesis (Fig. 4*C*). By contrast, when we treated *rde-1(flexon)* L4 larvae, all of their progeny hatched (Fig. 4*C*).

Similarly, when we performed *hlh-2(L1-RNAi)* on N2 larvae, we observed highly penetrant sterility, which was not observed when *hlh-2(L1-RNAi)* was performed on *rde-1(flexon)* hermaphrodites

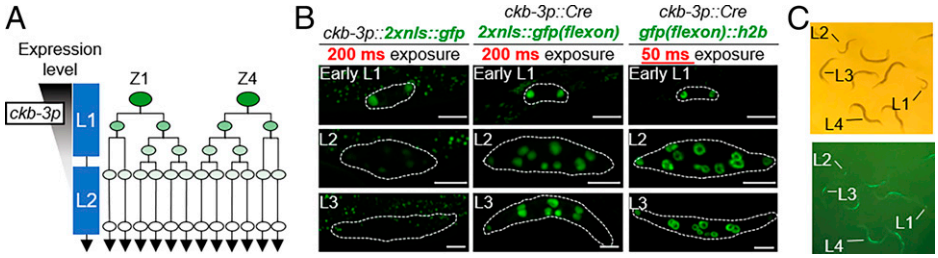

Fig. 2. The Flexon approach enables strong, persistent expression of GFP in all cells of the somatic gonad lineage. (*A*) *ckb-3p* drives expression of a high level of GFP specifically in the somatic gonad precursor cells Z1 and Z4 (29), but the level of GFP diminishes rapidly as the lineage progresses (see *B*, *Left* column). (*B*) GFP fluorescence from the transgene *arTi433[ckb-3p::2xnls::gfp]* (*Left* column) is dimmer and does not persist as long as GFP fluorescence from *arTi435[rps-27p::2xnls::gfp(flexon)]* when the *flexon* excision is mediated by a *ckb-3p::Cre* driver (*arTi237*; *Middle* column; *Materials and Methods*), as seen in photomicrographs taken at the same exposure time and imaging parameters. Stabilization of GFP using a histone tag (*arTi361[rps-27p::gfp(flexon)::h2b]; Right* column) results in bright expression visible at a lower exposure time than *2xnls::gfp*. (Scale bars, 10 μm.) (*C*) GFP(*flexon*)::histone in the presence of *ckb-3p::Cre* is visible on the dissecting scope at all larval stages. (Magnification, 50×.)

(Fig. 4*C*). Treated N2 larvae also displayed a highly penetrant lack of gonad arm extension (Fig. 4*C*), whereas the treated *rde-1(flexon)* larvae had normal gonad arms, with a single exception of an individual that had one normal and one abnormal gonad arm that extended but did not turn, consistent with reduced *hlh-2* activity after the DTCs had formed (42). Similarly, RNAi directed against *hlh-12*, which encodes the dimerization partner for HLH-2 for gonad arm extension (43), had a low proportion of "escapers": 1/104 (1%) gonad arms of treated *rde-1(flexon)* L1 larvae had a DTC with abnormal extension. Because most animals are unaffected, we infer that the *rde-1(flexon)* allele strongly abrogates *rde-1* activity, but the low proportion of escapers suggests that it may not be a true null allele. While there may be some situations in which a low background of residual *rde-1* activity may be problematic (39), we demonstrate below that it is eminently feasible to use *rde-1(flexon)* for tissue-specific RNAi.

We also tested two additional genes that have a cellular focus in tissues other than the somatic gonad: *dpy-10*, a cuticle collagen (44), and *pos-1*, an RNA-binding protein required for lineage specification in the early embryo (45). All progeny of treated N2 hermaphrodites displayed the expected phenotype: a Dumpy body shape for *dpy-10(RNAi)* (84/84) and embryonic lethal progeny for *pos-1(RNAi)* (716/716 arrested embryos). By contrast, the progeny of treated *rde-1(flexon)* hermaphrodites were generally unaffected: for *dpy-10(RNAi)*, 0/462 progeny were Dpy, and for *pos-1(RNAi)*, 4/604 arrested embryos were observed (we did not examine these arrested embryos for specific *pos-1*–associated defects). These results support the inference from *hlh-2(RNAi)* that insertion of the *flexon* into *rde-1* severely compromises its activity.

Test of endogenous* rde-1(flexon) *for tissue-specific RNAi in the somatic gonad. We tested whether restoring *rde-1* function specifically to the somatic gonad via excision of the *flexon* using the *ckb-3p::Cre* driver would result in highly penetrant, gonad abnormalities. As Cre is expressed in Z1 and Z4, we would expect that RNAi would be restored prior to the birth and specification of the DTCs. Indeed, *hlh-2(L1-RNAi)* of *rde-1(flexon); ckb-3p::Cre* resulted in sterility and lack of gonad arms, indicating that RNAi was efficiently restored by excision of the *flexon* (Fig. 4*C*). Moreover, all progeny of *hlh-2(L4-RNAi)* of *rde-1(flexon); ckb-3p::Cre* hermaphrodites survived (Fig. 4*C*), indicating that restoration of RNAi was specific to the gonad.

The observed bypass of embryonic lethality by *hlh-2(RNAi)* is strong evidence that restoration of RNAi by the *ckb-3p::Cre* driver is limited to the gonad. We corroborated this inference by performing *dpy-10* and *pos-1* RNAi on the *rde-1(flexon); ckb-3p::Cre* strain: 555/556 *dpy-10(RNAi)* individuals were non-Dpy and 424/433 progeny of *pos-1(RNAi)* hermaphrodites were viable, indicating that RNAi had not been restored to the hypodermis and germ line.

Tissue-specific restoration of* rde-1 *activity to body wall muscle. We performed an additional test of tissue-specific RNAi by restoring *rde-1* activity to the body wall muscles using *hlh-1p::Cre*, which drives excision in the MS muscle founder cell lineage (46–48), and performing RNAi against *unc-22*, which encodes the body wall muscle structural protein Twitchin/Titin (49). *unc-22(RNAi)* causes a fully penetrant Twitcher phenotype

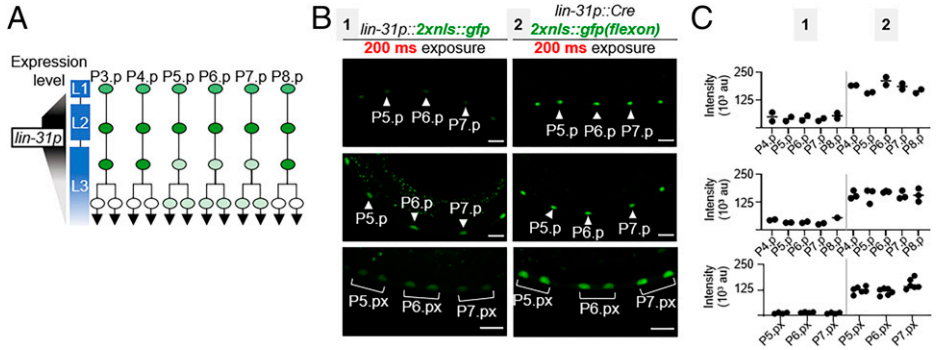

Fig. 3. The Flexon approach enables strong, persistent expression of GFP in the vulval precursor cell (VPC) lineages. (*A*) The *lin-31p* regulatory sequence drives expression of GFP in all VPCs in late L1 and L2, but GFP level becomes visibly nonuniform during vulval fate patterning in L3 and wanes as the lineages progress (34–36) (see *B*, *Left* column). (*B*) Photomicrographs of *arTi434[lin-31p::2xnls::gfp]* (*Left* column, genotype 1), showing dynamic expression pattern of *lin-31p* schematized in *A*. By contrast, GFP fluorescence intensity from *arTi435[rps-27p::2xnls::gfp(flexon)]* (*Right* column, genotype 2) is higher starting early in development and persists strongly throughout the VPC lineages. These *flexon* excisions were mediated by the VPC Cre driver *arTi381[lin-31p::Cre]*. (Scale bars, 10 μm.) (*C*) Quantitation of several individuals of genotypes 1 and 2 shown in *B*. Each dot represents one cell of one animal.

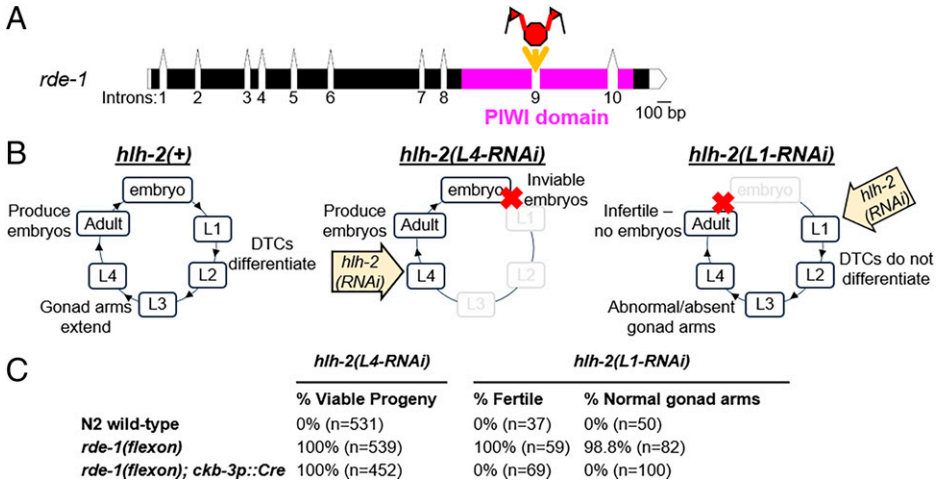

Fig. 4. Tissue-specific RNAi using the endogenous *rde-1(flexon)* allele. (*A*) The ninth intron of the endogenous *rde-1* locus was replaced with a *flexon* to generate *rde-1(ar660)*. (Scale bar, 100 bp.) White boxes in sequence indicate UTRs. The gene graphic was made using http://wormweb.org/exonintron. (*B*) *hlh-2* is required for viable embryogenesis and for the specification and function of the distal tip cells (DTCs) of the gonad, which lead proper gonad arm extension and maintain germline proliferation (*Left*). When N2 wild-type hermaphrodites are exposed to *hlh-2* RNAi beginning in the L4 larval stage *[hlh-2(L4-RNAi)]*, their progeny arrest during embryogenesis (*Middle*). When they are exposed to *hlh-2* RNAi beginning in the L1 stage *[hlh-2(L1-RNAi)]* (*Right*), the treated hermaphrodites are sterile and have improper gonad morphology due to failures in DTC differentiation and function. (*C*) Phenotypes caused by targeting *hlh-2* by RNAi. For *hlh-2(L4-RNAi)*, the % viable progeny was assessed by counting the number of dead eggs and moving larval progeny produced by treated hermaphrodites. For *hlh-2(L1-RNAi)*, fertility was assessed by the presence of eggs on the plate or in the gonad, and each gonad arm was assessed in adults for presence, shape, and length. See *Materials and Methods* for further details.

when N2 (15/15) or *rde-1(ar660);hlh-1p::Cre* hermaphrodites (16/16) are treated, but does not cause a phenotype when *rde-1(ar660)* (0/16) or *rde-1(ar660);ckb-3p::Cre* (0/13) hermaphrodites are treated. Thus, tissue-specific RNAi was achieved in this additional cell context.

Final comments on *rde-1(flexon)*. We have provided proof of concept that the Flexon approach is applicable to endogenous genes, the main goal of this experiment, by showing that insertion of a *flexon* strongly reduces *rde-1* gene activity and that excision of the *flexon* after expression of tissue-specific Cre drivers restores gene activity. Our analysis suggests that *rde-1(ar660[flexon])* is a strong loss-of-function allele that should facilitate many tissue-specific RNAi applications and be a valuable addition to the tissue-specific RNAi toolkit for *C. elegans*. It should be straightforward to assess the feasibility of using *rde-1(ar660[flexon])* for any specific purpose by performing RNAi in the absence of a Cre driver at the outset of a study to confirm that the associated phenotype is not observed from potential low-level leaky expression at significant penetrance (as indeed would also be necessary for transgene rescue–based approaches).

Discussion

Stop cassettes are a versatile method for achieving conditional gene expression, a powerful approach for genetic analysis of any biological process. Here, we developed and tested a stop cassette we call a *flexon*, composed of an artificial exon flanked by artificial introns and site-specific recombinase sequences. A *flexon* can be flexibly positioned in a gene to prevent translation of its protein product until it is excised by tissue-specific expression of the cognate recombinase. We have provided a prototype for achieving strong, tissue-specific expression of a desired protein using two transgenes, one using a weak tissue-specific promoter to drive Cre and the other a strong promoter with a *gfp(flexon)*. We also inserted a *flexon* into the endogenous locus for *rde-1*, a gene required for RNAi, and showed that gene function was abrogated in the absence of Cre, but restored in specific tissues in the presence of a Cre driver. While it was used here as proof of concept for *flexon* function in an endogenous gene context, the *rde-1(flexon)* allele will be useful for tissue-specific RNAi in *C. elegans*. Here, we first generalize the design consideration for other *flexon* cassettes and then provide further examples of how the Flexon approach could be adapted to improve the efficiency of commonly used genetic tools and for additional genetic approaches in *C. elegans* and other experimental systems. Finally, we describe some potential limitations that should be borne in mind when applying the Flexon approach.

Design Considerations for Other *flexon* Cassettes. In principle, a *flexon* may be used with any protein-coding gene. In Fig. 5*A*, we show several adjustments that may be made to the *flexon* cassette we used here and highlight here and in the *SI Appendix* considerations for designing a *flexon*. In addition to cassette adjustments, when used in a transgene, different ubiquitous or more restricted promoters may be used to tune the level or tissue in which the *flexon*-containing construct is expressed after excision of the cassette (Fig. 5*B*; *SI Appendix*, Fig. S3).

1) The artificial exon sequence design should be tested in silico by conceptual translation to ensure that it 1) causes a frameshift downstream and 2) introduces stop codons in all three reading frames. The exon design used in this study contains stop codons in two reading frames within the exon; stop codons in the third reading frame were generated in downstream exons by the frameshift. The exon sequence may be modified to include additional out-of-frame stop codons within the exon if necessary.
2) The specific pair of *lox* sequences selected to flank the exon can be chosen to allow for the possibility to excise multiple *flexon* cassettes simultaneously or to guard against causing intergenic DNA recombination in the presence of other genes that have *loxP*, *loxN*, or *lox551* sequences (such as the loxP scar left from the self-excising cassette method of genome engineering in *C. elegans*) (23). Alternatively, *frt* or other site-specific recombinase sequences can be used in place of *lox* sequences for spatiotemporal control of recombination and/or for differential control when combining different *flexon*-containing transgenes.

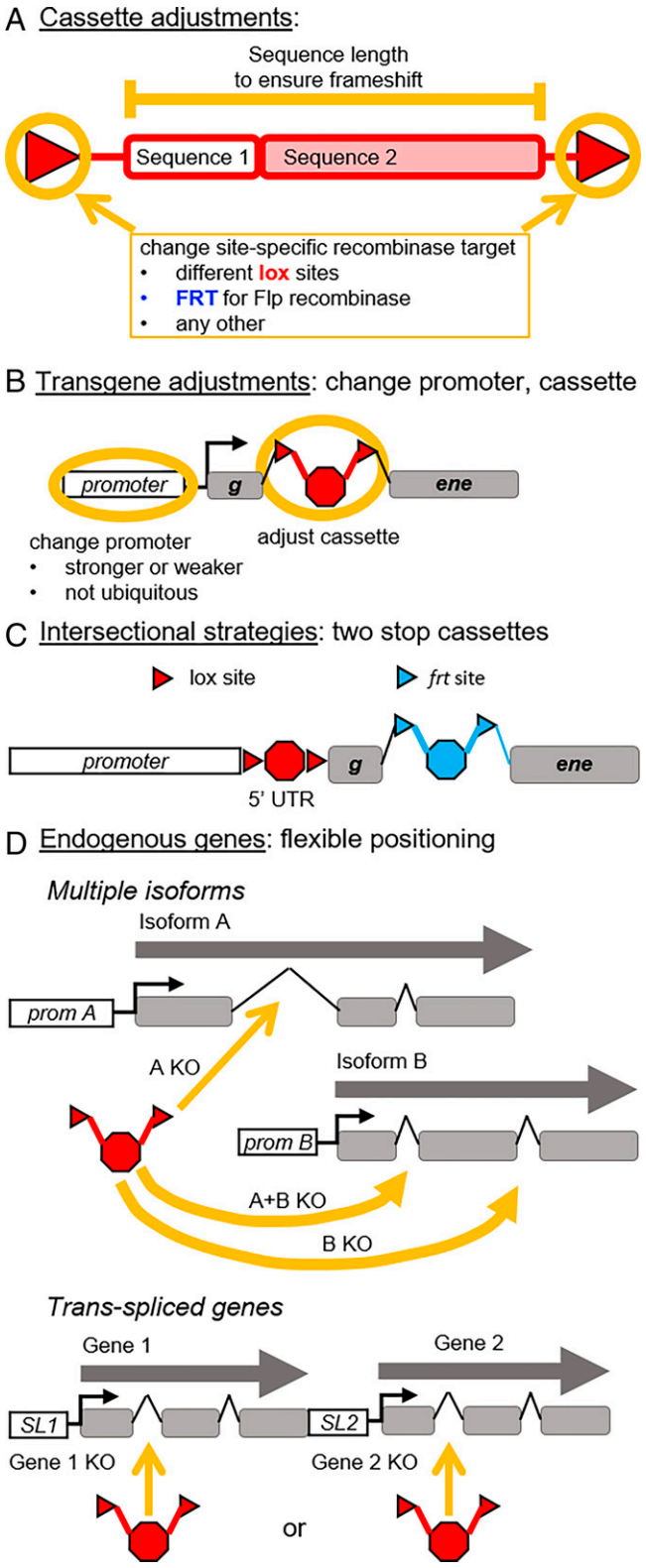

Fig. 5. Potential adjustments to the *flexon* design and additional applications. The Flexon system is tunable and may be incorporated into transgenes or endogenous loci to enable or improve genetic tools and approaches for manipulating gene activity as well as to mark lineages. Adjustments to the design for specific purposes (*A* and *B*) and some potential applications (*C* and *D*) are diagrammed here and described in the text.

3) Insertion of a *flexon* into an exon can be achieved by appending a splice donor site upstream of the first *lox* sequence and a splice acceptor sequence downstream of the second *lox* site. The introns here may be optimized in length or content for high splicing efficiency in alternate applications within *C. elegans* or for other organisms (*SI Appendix*).
4) When information about protein functional domains is available, it is preferable to insert the *flexon* such that expression from potential cryptic, downstream start sites would not result in an active protein.

Once a *flexon* has been designed and the desired insertion obtained, it is important to assess how well gene expression or activity has been abrogated by insertion of the *flexon* as an important control for tissue-specific excision experiments (*Potential Limitations*).

Potential Applications Facilitated by Incorporating a *flexon* into Endogenous Genes or Transgenes. The Flexon approach may be incorporated into many different established strategies for manipulating gene activity or expression. We give some examples here, emphasizing *C. elegans* but applicable to other experimental systems.

Increasing the Level of Limiting Effectors for Tissue-Specific Protein Degradation. Targeted protein degradation using natural degron/ubiquitin ligase pairs is a powerful method for studying gene function. Several degron/ubiquitin ligase pairs have been successfully used in *C. elegans*: the TIR1/AID (Auxin-Inducible Degron) system (applied to *C. elegans* in ref. 50), the ZIF-1/ZF1 system (51), and converting GFP itself into a degron by replacing the interaction domain of an E3 ubiquitin ligase with an anti-GFP nanobody (52). However, the amount of the ubiquitin ligase expressed has been reported to be limiting for degradation (53–55), so we anticipate that the Flexon approach will facilitate such manipulations by enabling stronger tissue-specific expression of the ubiquitin ligase. Furthermore, by using different *lox* variants, Cre can be used to delete a floxed, degron-tagged gene while simultaneously using a *ubiquitin ligase(flexon)* to quickly eliminate perduring protein, a strategy that has been demonstrated to be effective when low residual protein levels obscure the null phenotype (2).

Intersectional Approaches to Conditional Gene Expression. One way to achieve specific gene expression is to use two different tissue-specific promoters that have overlapping sites of expression to drive different recombinases, e.g., combining the Cre and Flp recombinases (56–58) (Fig. 5*C*). The flexible placement of the *flexon* (Fig. 5*D*) may facilitate the use of such intersectional strategies. Combinatorial recombinase approaches have been used for marking specific cell types and lineages in mice (reviewed in ref. 59); in *C. elegans*, these approaches may be used to generate GFP lineage markers that require lower intensity and exposure to visualize, avoiding damage from blue-light overexposure (60, 61).

Engineering Genomic Loci. For engineering genomic loci, the flexibility in placement of a *flexon* offers several potential advantages over stop cassettes that are placed in a 5′ UTR. First, the Flexon approach facilitates the engineering of conditional alleles for single or multiple isoforms (Fig. 5*D*). Second, the flexible placement reduces the chance of disrupting uncharacterized but important regulatory sequences in the 5′ UTR by the single recombination site "scar" left after excision of the cassette. Third, in many cases introns are better defined than 5′ UTRs, especially in *C. elegans* where about 84% of genes are trans-spliced by the addition of a splice-leader sequence to the 5′ end of pre-mRNAs (62), and about 15% of genes are expressed from operons, in which a polycistronic pre-mRNA is processed into separate transcripts by trans-splicing of the downstream gene (63), with the trans-splice

acceptor for the downstream gene embedded in a relatively short sequence that also contains a 3′ UTR for the upstream gene. Thus, a *flexon* can be inserted into a trans-spliced gene, or into either gene of an operon, without potentially compromising regulatory sequences (Fig. 5*D*).

Finally, we note that manipulating endogenous gene expression using the Flexon approach offers an alternative to transgene-based methods for assessing tissue-specific rescue and creating genetic mosaics that may be advantageous in certain situations. For example, transgenes used for conventional tissue-specific rescue may not be expressed at endogenous levels, and when genes have multiple isoforms, the isoform selected may influence the results. By contrast, insertion of a *flexon* into an intron of an endogenous gene will allow for all isoforms that share that intron to be expressed under control of its natural regulatory elements after excision using a tissue-specific Cre driver (Fig. 5*D*).

Potential Limitations. Although the Flexon approach addresses some of the issues that have been observed with traditional lox-stop-lox, it shares other limitations inherent to any stop cassette method. One is that site-specific recombination is irreversible and therefore cannot be used for dynamic control of gene expression by itself, although it may facilitate the implementation of dynamic methods such as AID, as described above. Another limitation is that transient or variable low-level expression that is not normally evident when the promoters are identified using fluorescent reporter genes may be more apparent when they are used to drive Cre (46), so tissue-specific promoters used to drive site-specific recombinases may not be as specific as desired. A third limitation is that expression in different cells of a tissue may be uneven shortly after recombination events due to asynchronous cassette excision or when occasionally excision does not occur on both chromosomes in a cell. However, recombination tends to be very efficient given the small size of the *flexon*, so for many applications, this limitation may not be an issue.

A final limitation shared with other stop cassette approaches is potential "leakiness." Although we have attempted to address the causes of leakiness in traditional lox-stop-lox while also implementing the advantages of the flexible insertion of the stop cassette that a *flexon* offers, there is still the potential for leaky expression from a fortuitous downstream translational start site or alternative splicing/exon skipping that excludes the *flexon* from the final mRNA transcript. Such exon skipping may account for the rare escapers we observed when evaluating *rde-1(flexon)* for abrogating RNAi, and may depend on the specific gene, the specific tissue, or the specific *flexon* design itself. For practical purposes, whether leakiness is a problem may be easily addressed by examining the phenotype of novel endogenous *flexon* alleles. If incomplete penetrance is an issue, repositioning the *flexon*, adding an additional *flexon,* or combining the Flexon approach with another conditional method such as AID (2) are possible approaches to reducing such background activity.

One other consideration must be borne in mind when manipulating endogenous genes: Insertion of a *flexon* will abrogate gene function, so if a lethal or sterile phenotype is anticipated, marked balancer chromosomes (64, 65) or rescuing transgenes (such as extrachromosomal arrays that can be readily eliminated) should be included to circumvent this complication.

Materials and Methods

***C. elegans* Strains.** *C. elegans* was grown on 6-cm nematode growth medium plates seeded with *Escherichia coli* OP50 and maintained at 20 °C. Strain N2 (wild type) (66) and two of the Cre drivers used in this study were previously described: *arTi237 [ckb-3p::Cre(opti)::tbb-2 3′ UTR] X* is a single-copy insertion transgene made as described in ref. 46 and mapped as part of this study, and *arTi235 [hlh-1::Cre(opti)::tbb-2 3′ UTR]* was also described in ref. 46. Cre(opti) refers to the codon-optimized Cre recombinase described previously (30). The generation of other single-copy insertion transgenes and the allele *rde-1(ar660[flexon])* is described below. The full genotypes of strains used in this study are listed in *SI Appendix*, Table S1.

Generation of Single-Copy Insertion Transgenes. The plasmids pHK001 [*rps-27p::gfp(flexon)::his-58::unc-54 3′ UTR*], pJS110 [*ckb-3p::2xnls::gfp::unc-54 3′ UTR*], pJS145 [*rps-27p::2xnls::gfp(flexon)::unc-54 3′ UTR*] (Addgene #179159), and pJS146 [*lin-31p::2xnls::gfp::unc-54 3′ UTR*] were made in a miniMos vector backbone [pCFJ910] (67) using Gibson Assembly (NEB) and confirmed by sequencing. pJS110, pJS145, and pJS146 contain a *C. elegans* codon-optimized GFP sequence tagged with an N-terminal SV40 and C-terminal *egl-13* nuclear localization sequences (*nls*), regulated by the neutral 3′ UTR from *unc-54* (68). pHK001 uses a *C. elegans* GFP sequence with slightly different codon optimization (23). Plasmids were injected into N2 hermaphrodites. Random, single-copy insertions were obtained and mapped using the standard protocol (67).

Generation of *rde-1(ar660)*, the Endogenous *rde-1(flexon)* Allele. The repair template plasmid pJS155 was made using Gibson cloning to insert the following sequences into a pBluescript vector: The final 500 bp of *rde-1* exon 9, a *flexon* cassette, and the first 500 bp of *rde-1* exon 10. The arrangement of the sequences in pJS155 will effectively replace the native intron 9 of *rde-1* with the *flexon* cassette when the plasmid is used as a repair template. Intron 9 lies between two exons that encode of the catalytic PIWI domain of RDE-1.

To generate *rde-1(ar660)*, an injection mix containing pJS155 (50 ng/μL) as the repair template and a crRNA (IDT; tgagtatttaaaagatctctgttttagagctatgct) was prepared according to an established protocol (69) and injected into the gonads of young adult N2 hermaphrodites. Animals with potential gene editing events were isolated according to the protocol, and animals homozygous for a correct *rde-1(ar660)* allele were confirmed through PCR genotyping and sequencing.

We note that we made another allele by replacing the second intron of the endogenous *rde-1* locus with a *flexon* cassette. In contrast to *rde-1(ar660)*, the allele resulting from this replacement had only a weak effect on *rde-1* function. Because the second intron is upstream of the exons for all the known functional domains of RDE-1, we interpret the weak phenotype as an indication that cryptic, in-frame ATG start sites downstream of the *flexon* allowed for the transcription of a mutant RDE-1 protein that retained significant activity. This concern was incorporated into Design Considerations for Other *flexon* Cassettes section, point 4, and reiterated in *SI Appendix*.

Microscopy. *C. elegans* larvae were imaged for fluorescence on a Zeiss AxioObserver Z1 inverted microscope with a 63×, 1.4 numerical aperture (NA) oil immersion objective equipped with a spinning disk, CSU-X1A, a laser bench rack, and a Photometrics Evolve Electron Multiplying Charge Coupled Device camera. For GFP fluorescent imaging, a 488-nm, 100-mW laser was used for excitation. Larvae were mounted onto 3% agar pads and immobilized with 10 mM levamisole.

Z stacks were collected from GS9684, GS9686, GS9691, GS9692, and GS9401 larvae (Figs. 2 and 3) with slices at 500-nm intervals and imaged for GFP fluorescence with the following parameters: 10% laser power, 200-ms exposure (or 50-ms exposure for GS9401), and 400 EM gain. For *SI Appendix*, Fig. S3, the same parameters were used, but the animal was imaged with a 40×, 1.4 NA oil immersion objective, and with 1,000-nm intervals between slices. For strains GS9684, GS9692, and GS9401, the number of slices used per larva varied with the size of the gonad to fully capture the nuclei of every somatic gonad cell present. The stage of the animal was determined by the number of somatic gonad cells and somatic gonad morphology. For GS9686 and GS9691, each stack contained 26 slices, which was sufficient to image the full volume of the nuclei of every VPC or VPC descendant. The stage of the animal was determined by the number of VPCs and somatic gonad morphology.

Z stacks were collected from GS9401 and GS9407 (*SI Appendix*, Fig. S1) with slices at 500-nm intervals and imaged for GFP fluorescence with the following parameters: 25% laser power, 500 EM gain, and the exposure time denoted in the figure. The number of slices used per larva varied with the size of the gonad to fully capture the nuclei of every somatic gonad cell present. The stage of the animal was determined by the number of somatic gonad cells and somatic gonad morphology.

Images in Fig. 2*C* were taken on a phone camera through the eyepiece of a Zeiss Discovery V.12 SteREO dissecting microscope, GFP470 filter, Schott ACE 1 fiber optic light source, and X-cite series 120Q fluorescent lamp illuminator. Animals to be imaged were placed on 60-mm plates filled with 1.75% agarose and then immobilized using 10 mM levamisole.

Image Quantification. Fluorescence intensity was quantified using FIJI (70, 71). Z stacks were sum projected for all slices containing cells of interest. Nuclei were manually segmented, and the mean green fluorescent background from

a random region outside of the animal was subtracted from the mean green fluorescent intensity of each nucleus.

RNAi. The following RNAi clones were used: pKMS1196, which contains the full-length *hlh*-2 cDNA (72), and commercially available library clones for *unc-22*, *pos-1*, *dpy-10*, and *hlh-12* (73). For feeding RNAi (37), plates were made using NGM with 6 mM Isopropyl beta-D-1-thiogalactopyranoside and 100 μM carbenicillin, and seeded with 70 μL of overnight culture of bacteria expressing a single RNAi clone. Experiments were performed at 25 °C.

To test for embryonic lethality of *hlh-2(RNAi)*, N2, GS9801, and GS9802 individual L4 larvae were placed onto RNAi plates and then removed after 1 d. The number of eggs and surviving larvae on each plate were counted immediately upon removal, and then the number of surviving larvae were counted 1 d later. To test for sterility of *hlh-2(RNAi)*, N2, GS9801, and GS9802 embryos were isolated using a standard bleaching protocol (74) and plated onto unseeded NGM plates. Larvae were allowed to hatch for 1 h, isolated onto RNAi plates, and then assessed for fertility by checking for the presence of progeny 4 d after plating (Fig. 4 *B* and *C*). To assess gonad arm morphology in *hlh-2(RNAi)* and *hlh-12(RNAi)*, N2, GS9801, and GS9802 embryos were isolated by bleaching, plated directly onto RNAi plates, and assessed for gonad arm phenotypes 2 d after plating. Assessed phenotypes included gonad arm absence, failure to extend, failure to turn, failure to extend back to the midpoint, and the presence of abnormal bulges. The gonad arms of N2 animals on *hlh-12(RNAi)* had a very high penetrance of morphological defects (47/48).

For *unc-22(RNAi)*, individual N2, GS9801, GS9802, and GS9831 embryos or L1 larvae were placed onto RNAi plates and assessed for twitching at the L4 stage. To determine the effect of RNAi against *dpy-10* and *pos-1*, individual N2, GS9801, and GS9802 L1 larvae were placed onto RNAi plates and removed 2 d later after laying eggs. The progeny were then assessed for phenotypes, dumpy for *dpy-10* RNAi and lethality for *pos-1* RNAi.

Data Availability. All study data are included in the article and/or *SI Appendix*.

ACKNOWLEDGMENTS. We thank Katherine Luo for generating *arTi381* and Jee Hun (Henry) Kim for help in generating *arTi361*. We also thank Michael Shen, Michelle Attner, and Catherine O'Keeffe for valuable comments on the manuscript prior to submission; Gary Struhl for valuable comments after revision; and Barth Grant, John Kim, and Ann Rougvie for critical feedback and helpful suggestions that greatly improved this work. This work was supported by R35GM131746 from the National Institute of General Medical Sciences (to I.G.) and F31EY030331 from the National Eye Institute (to J.M.S.). J.M.S. was also supported by Training Grant T32GM008798. Some strains were provided by the *Caenorhabditis* Genetics Center, which is funded by NIH Office of Research Infrastructure Programs (P40 OD010440).

1. M. Lakso *et al.*, Targeted oncogene activation by site-specific recombination in transgenic mice. *Proc. Natl. Acad. Sci. U.S.A.* **89**, 6232–6236 (1992).
2. A. van der Vaart, M. Godfrey, V. Portegijs, S. van den Heuvel, Dose-dependent functions of SWI/SNF BAF in permitting and inhibiting cell proliferation in vivo. *Sci. Adv.* **6**, eaay3823 (2020).
3. E. L. Jackson *et al.*, Analysis of lung tumor initiation and progression using conditional expression of oncogenic K-ras. *Genes Dev.* **15**, 3243–3248 (2001).
4. I. H. Maxwell, G. S. Harrison, W. M. Wood, F. Maxwell, A DNA cassette containing a trimerized SV40 polyadenylation signal which efficiently blocks spurious plasmid-initiated transcription. *Biotechniques* **7**, 276–280 (1989).
5. L. Madisen *et al.*, A robust and high-throughput Cre reporting and characterization system for the whole mouse brain. *Nat. Neurosci.* **13**, 133–140 (2010).
6. C. J. Potter, B. Tasic, E. V. Russler, L. Liang, L. Luo, The Q system: A repressible binary system for transgene expression, lineage tracing, and mosaic analysis. *Cell* **141**, 536–548 (2010).
7. G. Struhl, K. Basler, Organizing activity of wingless protein in Drosophila. *Cell* **72**, 527–540 (1993).
8. K. Basler, G. Struhl, Compartment boundaries and the control of Drosophila limb pattern by hedgehog protein. *Nature* **368**, 208–214 (1994).
9. V. Cardot-Ruffino *et al.*, Generation of a conditional Flpo/FRT mouse model expressing constitutively active TGFβ in fibroblasts. *Sci. Rep.* **10**, 1–13 (2020).
10. S. O'Gorman, D. T. Fox, G. M. Wahl, Recombinase-mediated gene activation and site-specific integration in mammalian cells. *Science* **251**, 1351–1355 (1991).
11. L. A. Lyznik, J. C. Mitchell, L. Hirayama, T. K. Hodges, Activity of yeast FLP recombinase in maize and rice protoplasts. *Nucleic Acids Res.* **21**, 969–975 (1993).
12. M. W. Davis, J. J. Morton, D. Carroll, E. M. Jorgensen, Gene activation using FLP recombinase in *C. elegans*. *PLoS Genet.* **4**, e1000028 (2008).
13. C. Muñoz-Jiménez *et al.*, An efficient FLP-based toolkit for spatiotemporal control of gene expression in *Caenorhabditis elegans*. *Genetics* **206**, 1763–1778 (2017).
14. E. Z. Macosko *et al.*, A hub-and-spoke circuit drives pheromone attraction and social behaviour in *C. elegans*. *Nature* **458**, 1171–1175 (2009).
15. R. Voutev, E. J. A. Hubbard, A "FLP-Out" system for controlled gene expression in *Caenorhabditis elegans*. *Genetics* **180**, 103–119 (2008).
16. G. Friedrich, P. Soriano, Promoter traps in embryonic stem cells: A genetic screen to identify and mutate developmental genes in mice. *Genes Dev.* **5**, 1513–1523 (1991).
17. H. Niwa, K. Yamamura, J. Miyazaki, Efficient selection for high-expression transfectants with a novel eukaryotic vector. *Gene* **108**, 193–199 (1991).
18. V. T. Chu *et al.*, Efficient generation of Rosa26 knock-in mice using CRISPR/Cas9 in C57BL/6 zygotes. *BMC Biotechnol.* **16**, 1–15 (2016).
19. C. Xiao *et al.*, MiR-150 controls B cell differentiation by targeting the transcription factor c-Myb. *Cell* **131**, 146–159 (2007).
20. P. Soriano, Generalized lacZ expression with the ROSA26 Cre reporter strain. *Nat. Genet.* **21**, 70–71 (1999).
21. A. M. Bapst, S. L. Dahl, T. Knöpfel, R. H. Wenger, Cre-mediated, loxP independent sequential recombination of a tripartite transcriptional stop cassette allows for partial read-through transcription. *Biochim. Biophys. Acta. Gene Regul. Mech.* **1863**, 194568 (2020).
22. J. A. Arribere, H. Kuroyanagi, H. A. Hundley, mRNA editing, processing and quality control in *Caenorhabditis elegans*. *Genetics* **215**, 531–568 (2020).
23. D. J. Dickinson, A. M. Pani, J. K. Heppert, C. D. Higgins, B. Goldstein, Streamlined genome engineering with a self-excising drug selection cassette. *Genetics* **200**, 1035–1049 (2015).
24. R. Thermann *et al.*, Binary specification of nonsense codons by splicing and cytoplasmic translation. *EMBO J.* **17**, 3484–3494 (1998).
25. J. Zhang, X. Sun, Y. Qian, J. P. LaDuca, L. E. Maquat, At least one intron is required for the nonsense-mediated decay of triosephosphate isomerase mRNA: A possible link between nuclear splicing and cytoplasmic translation. *Mol. Cell. Biol.* **18**, 5272–5283 (1998).
26. C. Merritt, D. Rasoloson, D. Ko, G. Seydoux, 3′ UTRs are the primary regulators of gene expression in the *C. elegans* germline. *Curr. Biol.* **18**, 1476–1482 (2008).
27. R. Giordano-Santini *et al.*, An antibiotic selection marker for nematode transgenesis. *Nat. Methods* **7**, 721–723 (2010).
28. J. Kimble, D. Hirsh, The postembryonic cell lineages of the hermaphrodite and male gonads in *Caenorhabditis elegans*. *Dev. Biol.* **70**, 396–417 (1979).
29. M. B. Kroetz, D. Zarkower, Cell-specific mRNA profiling of the *Caenorhabditis elegans* somatic gonadal precursor cells identifies suites of sex-biased and gonad-enriched transcripts. *G3* **5**, 2831–2841 (2015).
30. S. Ruijtenberg, S. van den Heuvel, G1/S inhibitors and the SWI/SNF complex control cell-cycle exit during muscle differentiation. *Cell* **162**, 300–313 (2015).
31. P. W. Sternberg, "Vulval development" in WormBook, *The Online Review of C. elegans Biology* (2005).
32. H. Shin, D. J. Reiner, The signaling network controlling *C. elegans* vulval cell fate patterning. *J. Dev. Biol.* **6**, 30 (2018).
33. K. Gauthier, C. E. Rocheleau, "*C. elegans* vulva induction: An in vivo model to study epidermal growth factor receptor signaling and trafficking" in *ErbB Receptor Signaling. Methods in Molecular Biology*, Z. Wang, Ed. (Humana Press, New York, NY, 2017), **vol. 1652**.
34. P. B. Tan, M. R. Lackner, S. K. Kim, MAP kinase signaling specificity mediated by the LIN-1 Ets/LIN-31 WH transcription factor complex during *C. elegans* vulval induction. *Cell* **93**, 569–580 (1998).
35. C. de la Cova, I. Greenwald, SEL-10/Fbw7-dependent negative feedback regulation of LIN-45/Braf signaling in *C. elegans* via a conserved phosphodegron. *Genes Dev.* **26**, 2524–2535 (2012).
36. K. L. Luo, R. S. Underwood, I. Greenwald, Positive autoregulation of *lag-1* in response to LIN-12 activation in cell fate decisions during *C. elegans* reproductive system development. *Development* **147**, dev193482 (2020).
37. L. Timmons, D. L. Court, A. Fire, Ingestion of bacterially expressed dsRNAs can produce specific and potent genetic interference in *Caenorhabditis elegans*. *Gene* **263**, 103–112 (2001).
38. H. Qadota *et al.*, Establishment of a tissue-specific RNAi system in *C. elegans*. *Gene* **400**, 166–173 (2007).
39. J. S. Watts *et al.*, New strains for tissue-specific RNAi studies in *Caenorhabditis elegans*. *G3* **10**, 4167–4176 (2020).
40. M. Krause *et al.*, A *C. elegans* E/Daughterless bHLH protein marks neuronal but not striated muscle development. *Development* **124**, 2179–2189 (1997).
41. R. S. Kamath, M. Martinez-Campos, P. Zipperlen, A. G. Fraser, J. Ahringer, Effectiveness of specific RNA-mediated interference through ingested double-stranded RNA in *Caenorhabditis elegans*. *Genome Biol.* **2**, research0002.0001 (2000).
42. X. Karp, I. Greenwald, Multiple roles for the E/Daughterless ortholog HLH-2 during *C. elegans* gonadogenesis. *Dev. Biol.* **272**, 460–469 (2004).
43. K. K. Tamai, K. Nishiwaki, bHLH transcription factors regulate organ morphogenesis via activation of an ADAMTS protease in *C. elegans*. *Dev. Biol.* **308**, 562–571 (2007).
44. A. D. Levy, J. Yang, J. M. Kramer, Molecular and genetic analyses of the *Caenorhabditis elegans* dpy-2 and dpy-10 collagen genes: A variety of molecular alterations affect organismal morphology. *Mol. Biol. Cell* **4**, 803–817 (1993).
45. H. Tabara, R. J. Hill, C. C. Mello, J. R. Priess, Y. Kohara, pos-1 encodes a cytoplasmic zinc-finger protein essential for germline specification in *C. elegans*. *Development* **126**, 1–11 (1999).
46. C. C. Tenen, I. Greenwald, Cell non-autonomous function of daf-18/PTEN in the somatic gonad coordinates somatic gonad and germline development in *C. elegans* dauer larvae. *Curr. Biol.* **29**, 1064–1072.e8 (2019).

47. M. Krause, S. W. Harrison, S.-Q. Xu, L. Chen, A. Fire, Elements regulating cell- and stage-specific expression of the *C. elegans* MyoD family homolog hlh-1. *Dev. Biol.* **166**, 133–148 (1994).
48. J. I. Murray *et al.*, Automated analysis of embryonic gene expression with cellular resolution in *C. elegans*. *Nat. Methods* **5**, 703–709 (2008).
49. D. G. Moerman, G. M. Benian, R. J. Barstead, L. A. Schriefer, R. H. Waterston, Identification and intracellular localization of the unc-22 gene product of *Caenorhabditis elegans*. *Genes Dev.* **2**, 93–105 (1988).
50. L. Zhang, J. D. Ward, Z. Cheng, A. F. Dernburg, The auxin-inducible degradation (AID) system enables versatile conditional protein depletion in *C. elegans*. *Development* **142**, 4374–4384 (2015).
51. S. T. Armenti, L. L. Lohmer, D. R. Sherwood, J. Nance, Repurposing an endogenous degradation system for rapid and targeted depletion of *C. elegans* proteins. *Development* **141**, 4640–4647 (2014).
52. S. Wang *et al.*, A toolkit for GFP-mediated tissue-specific protein degradation in *C. elegans*. *Development* **144**, 2694–2701 (2017).
53. U. Aghayeva *et al.*, DAF-16/FoxO and DAF-12/VDR control cellular plasticity both cell-autonomously and via interorgan signaling. *PLoS Biol.* **19**, e3001204 (2021).
54. G. E. Ashley *et al.*, An expanded auxin-inducible degron toolkit for *Caenorhabditis elegans*. *Genetics* **217**, iyab006 (2021).
55. F. dos Santos Maraschin, J. Memelink, R. Offringa, Auxin-induced, SCF(TIR1)-mediated poly-ubiquitination marks AUX/IAA proteins for degradation. *Plant J.* **59**, 100–109 (2009).
56. R. Awatramani, P. Soriano, C. Rodriguez, J. J. Mai, S. M. Dymecki, Cryptic boundaries in roof plate and choroid plexus identified by intersectional gene activation. *Nat. Genet.* **35**, 70–75 (2003).
57. K. Liu, H. Jin, B. Zhou, Genetic lineage tracing with multiple DNA recombinases: A user's guide for conducting more precise cell fate mapping studies. *J. Biol. Chem.* **295**, 6413–6424 (2020).
58. K. Anastassiadis, S. Glaser, A. Kranz, K. Bernhardt, A. F. Stewart, "A practical summary of site-specific recombination, conditional mutagenesis, and tamoxifen induction of CreERT2" in *Methods in Enzymology*, P. M. Wassarman, P. M. Soriano, Eds. (Academic Press, 2010), **vol. 477**, pp. 109–123.
59. S. M. Dymecki, R. S. Ray, J. C. Kim, "Mapping cell fate and function using recombinase-based intersectional strategies" in *Methods in Enzymology*, P. M. Wassarman, P. M. Soriano, Eds. (Academic Press, 2010), **vol. 477**, pp. 183–213.
60. S. L. Edwards *et al.*, A novel molecular solution for ultraviolet light detection in *Caenorhabditis elegans*. *PLoS Biol.* **6**, e198 (2008).
61. A. Ward, J. Liu, Z. Feng, X. Z. S. Xu, Light-sensitive neurons and channels mediate phototaxis in *C. elegans*. *Nat. Neurosci.* **11**, 916–922 (2008).
62. N. J. Tourasse, J. R. M. Millet, D. Dupuy, Quantitative RNA-seq meta-analysis of alternative exon usage in *C. elegans*. *Genome Res.* **27**, 2120–2128 (2017).
63. M. A. Allen, L. W. Hillier, R. H. Waterston, T. Blumenthal, A global analysis of *C. elegans* trans-splicing. *Genome Res.* **21**, 255–264 (2011).
64. K. Dejima *et al.*, An aneuploidy-free and structurally defined balancer chromosome toolkit for *Caenorhabditis elegans*. *Cell Rep.* **22**, 232–241 (2018).
65. S. Iwata, S. Yoshina, Y. Suehiro, S. Hori, S. Mitani, Engineering new balancer chromosomes in *C. elegans* via CRISPR/Cas9. *Sci. Rep.* **6**, 1–6 (2016).
66. S. Brenner, The genetics of *Caenorhabditis elegans*. *Genetics* **77**, 71–94 (1974).
67. C. Frøkjær-Jensen *et al.*, Random and targeted transgene insertion in *Caenorhabditis elegans* using a modified Mos1 transposon. *Nat. Methods* **11**, 529–534 (2014).
68. R. Hunt-Newbury *et al.*, High-throughput in vivo analysis of gene expression in *Caenorhabditis elegans*. *PLoS Biol.* **5**, e237 (2007).
69. K. S. Ghanta, C. C. Mello, Melting dsDNA donor molecules greatly improves precision genome editing in *Caenorhabditis elegans*. *Genetics* **216**, 643–650 (2020).
70. M. Linkert *et al.*, Metadata matters: Access to image data in the real world. *J. Cell Biol.* **189**, 777–782 (2010).
71. J. Schindelin *et al.*, Fiji: An open-source platform for biological-image analysis. *Nat. Methods* **9**, 676–682 (2012).
72. X. Karp, I. Greenwald, Post-transcriptional regulation of the E/Daughterless ortholog HLH-2, negative feedback, and birth order bias during the AC/VU decision in *C. elegans*. *Genes Dev.* **17**, 3100–3111 (2003).
73. R. S. Kamath *et al.*, Systematic functional analysis of the *Caenorhabditis elegans* genome using RNAi. *Nature* **421**, 231–237 (2003).
74. T. Stiernagle, "Maintenance of *C. elegans*" in WormBook, The *C. elegans* Research Community (2006).